Articles

Rotational Contour Analysis of the Vibronic Bands in the High Resolution Emission Spectra of the Benzyl Radical

Iek Soon Choi, Myoung Sun Han, and Sang Kuk Lee*

Department of Chemistry, College of Natural Sciences, Pusan National University, Pusan 609-735, Korea
Received November 28, 1995

The $6a_1^0$ and $6b_1^0$ vibronic bands in the 1^2A_2-1^2B_2 electronic transition of the emission spectra of the benzyl radical obtained using a high resolution Fourier transform spectrometer are rotationally analyzed. The observed rotational contours were fitted by computer simulated rotational contours, providing determination of the variations, ΔA, ΔB, and ΔC of the rotational constants accompanying the vibronic transitions corresponding to each band. The molecular rotational constants A, B, and C are revised for the upper state and for the two lower states, respectively.

Introduction

The benzyl radical, the prototype of aromatic radicals, has been the subject of numerous experimental and theoretical works in recent years. The first electronic spectrum of benzyl radical was obtained in emission near 450 nm by Schüler *et al.*[1] A few years later, Porter and coworkers also identified the 305 nm band[2] as well as the 450 nm band[3] from the electronic absorption spectra employing the flash photolysis technique. The visible band system is, by far, the most widely studied of all the observed vibronic transitions of the benzyl radical. Cossart-Magos and Leach[4,5] have determined the symmetry of the excited state at 450 nm from the analysis of the rotational contour of the vibronic band. Cossart-Magos group[6,7] have also analyzed the rotational contours of the vibronic bands of the room temperature emission spectra of the benzyl radical and xylyl radicals. Recently, Carrick and Selco[8] have tried to determine the rotational constants of the benzyl radical in the visible region with a high resolution emission spectra. However, the ratio of signal to noise of the spectra was not enough to show the rotational fine structure clearly.

Laser induced fluorescence method[9~12] has been used to examine the vibronic coupling of two quasi-degenerate excited electronic states of the benzyl radical in the visible spectral region. Very recently, Miller's group has provided rotational constants of the benzyl radical[13] from the fit of the rotationally resolved LIF excitation spectra to a rigid asymmetric rotor Hamiltonian. A similar study has been also performed by Fukushima and Obi[14,15] for the rotationally resolved LIF excitation and dispersed fluorescence spectra.

As for the theoretical works, Longuet-Higgins and Pople[16] made the first attempt to explain the electronic structure of the benzyl radical observed at 450 nm. Since then, there have been numerous *ab initio* calculations.[17,18] The latest 'state-of-the art' *ab initio* calculation has been carried out by Rice *et al.*[19] Recently, Negri *et al.*[20] have made a theoretical publication about the vibronic coupling between the two lowest excited electronic states of the molecules.

In the present study, we report the analysis of the rotational contours of the $6a_1^0$ and $6b_1^0$ vibronic bands in the high resolution emission spectra of the benzyl radical which was generated in a jet by expansion with an inert buffer gas He from a high voltage dc discharge of the toluene.

Experimental details

The observation of high resolution emission spectra of benzyl radical in a jet has been carried out using the experimental apparatus which is similar to those previously employed.[21,22] The details of the experiment and the spectra observed have been already published.[23]

The benzyl radical was produced in a jet by an electric dc discharge of the gas mixture of the buffer gas He and the precursor toluene. For the electronic emission spectra, the Fourier transform spectrometer equipped with a Quartz-vis beamsplitter, a home-made ac preamplifier, and a PMT detector (Hamamatsu model 1P28) for photon counter has been employed.

The signal to noise ratio of the spectra observed was substantially improved with a 10 nm bandpass narrow band interference optical filter centered at 470 nm which blocks off very strong fluorescence from the carrier gas.

Initially, the survey scans were tried at 2.0 cm^{-1} resolution. After the experimental conditions for the $6a_1^0$ and $6b_1^0$ vibronic bands were optimized, the high resolution spectra were obtained at the resolution of 0.05 cm^{-1} over the region from 16000 to 25000 cm^{-1}. A total of 250 scans have been added together over 2 hrs. to obtain the final spectra shown in Figures 1 and 2. The accuracy of the frequency is believed to be better than 0.005 cm^{-1} from the calibration with I_2 transitions.[24]

Result and Discussions

The benzyl radical belongs to a planar C_{2v} point group with seven π delocalized electrons from the carbon atoms and thus has seven molecular orbitals (MOs) arising from the seven atomic orbitals (AOs).[25] The seven MOs are represented by $1b_2$, $2b_2$, $1a_2$, $3b_2$, $2a_2$, $4b_2$, $5b_2$. According to the

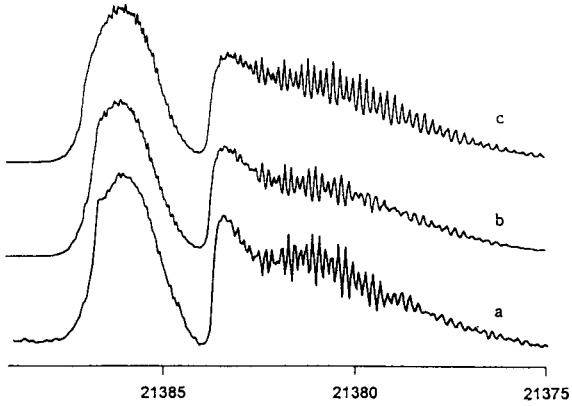

Figure 1. Comparison of the observed with calculated rotational band contour of the $6b_1^0$ vibronic transition of the benzyl radical. The observed spectrum (a) was obtained in emission using a Fourier transform spectrometer at the resolution of 0.07 cm^{-1}, while the simulated spectra (b) and (c) were calculated using a standard rigid asymmetric rotor program with the data given in Table 2 and in Ref. [8] at 50 K, respectively.

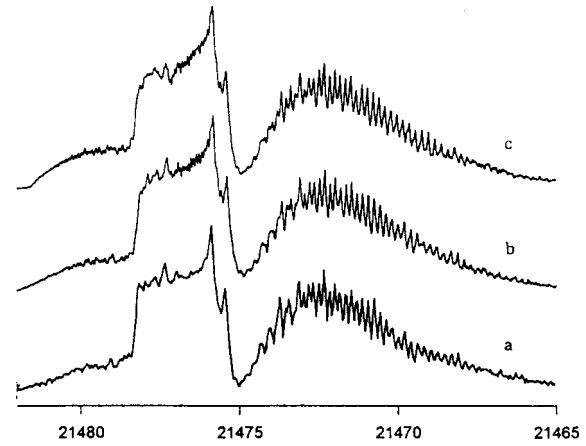

Figure 2. Comparison of the observed with calculated rotational band contour of the $6a_1^0$ vibronic transition of the benzyl radical. The observed spectrum (a) was obtained in emission using a Fourier transform spectrometer at the resolution of 0.07 cm^{-1}, while the simulated spectra (b) and (c) were calculated using a standard rigid asymmetric rotor program with the data given in Table 2 and in Ref. [8] at 50 K, respectrively.

Hückel π electron theory, the $3b_2$ MO belongs to nonbonding, the three MO's ($1b_2$, $2b_2$, and $1a_2$) below $3b_2$ in energy are bonding and the higher ones ($2a_2$, $4b_2$, and $5b_2$) antibonding. Thus the electron configuration of the ground state (X^2B_2) is

$(1b_2)^2\ (2b_2)^2\ (1a_2)^2\ (3b_2)^1\ (2a_2)^0\ (4b_2)^0\ (5b_2)^0$.

For the lowest excited electronic states, there are two possible isoenergetic one electron promotions involving a_2 MOs, resulting in a degenerate pair of $^2A_2$ states. However, in the presence of configuration interaction (CI), the two degenerate pairs of zeroth order electronic states of the same symmetry interact and repel strongly, splitting widely the initially degenerate pairs. The lower part of the $^2A_2$ states, 1^2A_2 is observed to lie at the 22002 cm^{-1} above the ground state (1^2B_2) and interacts vibronically with nearby 2^2B_2 electronic state.[26]

Table 1. Band Types of the Benzyl Radical according to Electronic Transition Assignment

Transitions	Band Types		
	0_0^0	$6a_1^0$	$6b_1^0$
1^2A_2-1^2B_2	type B	type B	type A
1^2B_2-1^2B_2	type A	type A	type B

The rotational contour of a vibronic band depends on the selection rules for the transition. Also, the detailed shape of the contour is a function of the the rotational constants A, B, and C in the ground or excited electronic state and the variations ΔA, ΔB, and ΔC of the constants in transition from one electronic state to the other state if the centrifugal distortion effect is neglected.

The selection rules for a particular vibronic transition of the asymmetric rotor are essentially determined by the direction of the transition moment with respect to the molecular framework. If the moment is directed along the *a*, *b*, or *c* principal axes, the resulting band contours will be type *A*, type *B*, or type *C*, respectively; hybrid band contours will appear if the transition moment has components in more than one axis direction. The selection rules $\Delta J = 0, \pm 1$ will be valid for all types of bands, but ΔK_a and ΔK_c will be different for the different band types. The selection rules are ΔK_a = even, ΔK_c = odd for type A band and ΔK_a = odd, ΔK_c = odd for type B band, ΔK_a = odd, ΔK_c = even for type C band, respectively.[27] The vibronic bands of benzyl radical discussed here will be type A or type B according to the two possible electronic transition assignments, as shown in Table 1.[5]

The benzyl radical has Ray's asymmetry parameter $\kappa \simeq -0.5$ in the ground state and this is not expected to change significantly in the first excited state (1^2A_2), thus it is closer to a prolate than to an oblate symmetric top in both electronic states.

According to the low resolution emission study,[26] the two strongest bands located at 21384 and 21475 cm^{-1} shown in Figures 1 and 2 were identified as the $6b_1^0$ and $6a_1^0$ vibronic bands in the 1^2A_2-1^2B_2 electronic transition of the benzyl radical, respectively.

Calculation Procedure

One of the main advantages in rotational contour analysis is that even in the absence of full rotational resolution, the rotational contour of the gas phase spectrum can be used to estimate the rotational temperature, as well as the change in the rotational constants during the electronic transition.

The simulated band contours were calculated using a standard rigid asymmetric rotor program ASYROT which was originally written by Birss *et al.*[28] and later modified to PC version by Judge.[29] The program was combined with a simple seven-point triangular line blending program for plotting the simulated spectrum.

In this calculation, the calculation time has been be dra-

matically reduced with two approximations: (1) cut off the reduced energy E (κ) matrices; (2) interpolation of rotational transition frequencies and intensities between a number of calculated values. Also, the spin splitting was neglected in both doublet electronic states so that the transition was treated formally as a singlet-singlet transition.

With modification of the program the maximum J value has been increased up to 100 and the symmetric rotor approximation was made for $K_a>70$ which are believed to be sufficient for the simulated spectra at low rotational temperature.

The ratio of the nuclear spin statistical weights K_a(even) /K_a(odd) is 7/9 for the zero vibrational level of an upper state of the $^2A_2$ electronic symmetry of $C_6H_5CH_2$ which is the common upper level of the two bands.[5] This ratio would be inversed if the upper state were of the $^2B_2$ symmetry, so that the intensity variations of the transitions involving upper state K_a levels of even and odd symmetry could provide a diagnostic tool for identification of the symmetry of upper electronic state. However, the different K_a subbranches could not be resolved from each other in our spectra. Thus, we considered the g multiplicity factor as being constant for all transition components of the vibronic band.

In emission experiment, the Boltzmann factor should be applied to the upper state of the transition. However, emission introduces an uncertainty in the source temperature, whereas in absorption studies on stable molecules the temperature can be well defined.[6] From the comparison of the spectra simulated with the spectra observed, the best agreement has been obtained with the rotational temperature of about 50 K. This is quite reasonable for our source by considering the experimental setup employed in this work.[30]

The spectral line profiles were considered to arise mainly from Doppler effects and were taken to be Gaussian. The Doppler width (FWHM) of the carrier gas He at rotational temperature of 50 K is equal to 0.0544 cm $^{-1}$, which is comparable to the resolution of 0.05 cm^{-1} of the spectrometer employed for the spectra. Consequently, a triangular line width (FWHM) of 0.05 cm $^{-1}$ was used in the calculations. The simulated spectra were constructed by adding the intensities of all points with the same frequency at 0.05 cm $^{-1}$ frequency intervals.

In this process, of course, all centrifugal distortion constants of the benzyl radical were neglected because they should affect transition energies by at the most only a few hundredths of a cm^{-1} in unfavorable circumstances. However, from the comparison between two spectra, we have found small differences in peak positions which indicate that the values of the rotational constants and the band origin should be revised.

We have initially attempted to determine the rotational constants by a least squares fit of the rotationally resolved frequencies to a standard asymmetric rotor Hamiltonian for all states embodied in the program. But, it was not possible to produce the observed bandshapes shown in Figures 1 and 2 with the rotational constants obtained by fitting due to the limited resolution of the rotational contours in the R branch.

Since bandshapes and contours are typically much more sensitive to the changes in the geometry associated with the transition rather than to their absolute values, we have tried to simulate the observed rotational contours with a "reasonable set" of rotational constants for each of the three states; a common excited state, two different ground states ($v_{6b}=1$ and $v_{6a}=1$), and with a variable temperature, T. The calculation was also incorporated with the appropriate rovibronic selection rules of type A and type B for the $6b_1^0$ and $6a_1^0$ vibronic bands, respectively. As shown in Figures 1 and 2, excellent agreement has been obtained between the observed and calculated rotational contours. Also, the simulated spectrum obtained using the data given by Carrick and Selco[8] was compared in Figures 1 and 2. The values of the rotational constants used for this calculation are presented in Table 2 and compared in Table 3 with those of the previous work during the vibronic transition. The changes in rotational constants upon transition are similar to both bands. The fact that ΔA is larger than ΔB or ΔC is in good agreements with those[5,8] reported previously.

Table 2. Rotational Constants of the $6a_1^0$ and $6b_1^0$ Vibronic Bands of the $1^2A_2 \rightarrow 1^2B_2$ Electronic transition of the Benzyl Radical used to produce the Simulated Spectra shown in Figures 2 and 3.[a]

	Lower state $6b_1^0$	Lower state $6a_1^0$	Upper state (1^2A_2)
A	0.184285	0.184480	0.180391
B	0.090088	0.090070	0.088448
C	0.060459	0.060347	0.059200
T	21383.782	21475.057	

[a] In units of cm^{-1}.

Table 3. Comparison of the Differences in Rotational Constants with the Values Reported Previously during the Transition[a,b]

	Present study		Previous study[c]	
	$6b_1^0$	$6a_1^0$	$6b_1^0$	$6a_1^0$
ΔA	−0.003894	−0.004089	−0.004722	−0.004629
B	−0.001640	−0.001622	−0.001561	−0.001461
C	−0.001259	−0.001147	−0.001117	−0.001109

[a] In units of cm^{-1}. [b] Difference between upper and lower rotational constants. [c] Ref. [8].

Summary

In the present study, we have analyzed the rotational contour of the $6b_1^0$ and $6a_1^0$ vibronic bands of the high resolution emission spectra of the benzyl radical in the 1^2A_2-1^2B_2 electronic transition. From the comparison of the spectra simulated with the spectra observed, the rotational constants and the band origin of benzyl radical have been revised.

Acknowledgment. This work was supported by the Korea Science and Engineering Foundation (Grant No. 951-0302-048-2).

References

1. Schüler, H.; Reinebeck, L.; Kaberle, A. R. *Z. Naturforsch.* **1952**, *79*, 421.
2. Porter, G.; Ward, B. *J. Chim. Phys.* **1964**, *61*, 102.

3. Porter, G.; Strachan, E. *Spectrochim. Acta* **1958**, *12*, 299.
4. Cossart-Magos, C.; Leach, S. *J. Chem. Phys.* **1976**, *64*, 4006.
5. Cossart-Magos, C.; Leach, S. *J. Chem. Phys.* **1972**, *56*, 1534.
6. Cossart-Magos, C.; Goetz, W. *J. Mol. Spectrosc.* **1986**, *115*, 366.
7. Cossart-Magos, C.; Cossart, D.; Leach, S. *Chem. Phys.* **1973**, *1*, 306.
8. Carrick, P. G.; Selco, J. I. *J. Mol. Spectrosc.* **1990**, *139*, 449.
9. Okamura, T.; Charlton, T. R.; Thrush, B. A. *Chem. Phys. Lett.* **1982**, *88*, 369.
10. Heaven, M.; DiMauro, L.; Miller, T. A. *Chem. Phys. Lett.* **1983**, *95*, 347.
11. Foster, S. C.; Miller, T. A. *J. Phys. Chem.* **1989**, *93*, 5986.
12. Brenner, D. M.; Smith, G. P.; Zare, R. N. *J. Am. Chem. Soc.* **1976**, *98*, 6707.
13. Lin, T.-Y. D.; Tan, X.-Q.; Cerny, T. M.; Williamson, J. M.; Cullin, D. W.; Miller, T. A. *Chem. Phys.* **1992**, *167*, 203.
14. Fukushima, M.; Obi, K. *J. Chem. Phys.* **1990**, *93*, 8488.
15. Fukushima, M.; Obi, K. *J. Chem. Phys.* **1992**, *96*, 4224.
16. Longuet-Higgins, H. C.; Pople, J. *Proc. Phys. Soc.* **1955**, *A68*, 591.
17. Schley, J. C.; Philips, D. H. *J. Chem. Phys.* **1968**, *49*, 3734.
18. Chang, H. M.; Jaffe, H. H. *Chem. Phys. Lett.* **1973**, *23*, 146.
19. Rice, J. E.; Handy, N. C.; Knocoles, P. J. *J. Chem. Soc., Faraday Trans.* **1987**, *II83*, 1643.
20. Negri, F.; Orlandi, G.; Zerbetto, F.; Zgierski, M. Z. *J. Chem. Phys.* **1990**, *93*, 600.
21. Lee, S. K. *Bull. Korean Chem. Soc.* **1993**, *14*, 340.
22. Suh, M. H.; Lee, S. K.; Rehfuss, B. D.; Miller, T. A.; Bondybey, V. E. *J. Phys. Chem.* **1991**, *95*, 2727.
23. Lee, S. K. *Bull. Korean Chem. Soc.* **1995**, *16*, 795.
24. Gerstenkorn, G.; Luc, P. *Rev. Phys. Appl.* **1979**, *14*, 791.
25. Roberts, J. D. *Notes on Molecular Orbital Calculations*; Benzamin, Inc.: New York, New York, 1962; p 105.
26. Selco, J. I.; Carrick, P. G. *J. Mol. Spectrosc.* **1989**, *137*, 13.
27. Towner, C. H.; Schawlow, A. L. *Microwave Spectroscopy*; McGraw-Hill: New York, New York, 1955.
28. Birss, F. W.; Ramsay, D. A. *Comput. Phys. Commun.* **1984**, *38*, 83.
29. Judge, R. H. *Comput. Phys. Commun.* **1987**, *47*, 361.
30. Lee, S. K. *Bull. Korean. Chem. Soc.* **1994**, *15*, 349.

Reduction of Nitrogen Oxides from Fuel Nitrogen in New Fuelling System

Young-Nam Chun and Jae-Ou Chae*

Department of Environmental Engineering, Chosun University, Kwangju 501-759, Korea
**Department of Mechanical Engineering, Inha University, Inchon 402-751, Korea*
Received March 25, 1996

The effects of NOx reduction by advanced fuel staging in a small scale combustor (6.6 kW_T) have been investigated using propane gas flames laden with ammonia as fuel-nitrogen. The variables which had the greatest influence on NOx reduction were temperature, reducing stoichiometry (relate to main combustion zone stoichimetry, air fraction and reburning fuel fraction) and residence time of reducing zone. NOx reduction was best at the reburning zone temperature of above 1,000 ℃ and reburning zone stoichiometry was 0.85. In terms of residence time of the reburning zone, NOx reduction was effective when burnout air was injected at the point where the reburning zone had been already established. In the advanced fuel staging NOx reduction was relatively large at the burning of higher Fuel-N concentration in the fuel. Under optimum reburning conditions, fuel nitrogen content had a relatively minor impact on reburning efficiency.

Introduction

Nitrogen oxides (NOx) has been recognized as air pollutants for decades due to its effects on human and animal health, damage to vegetation and the role of NOx in producing smog.

Staged combustion has been demonstrated as an effective method for reducing nitrogen oxides emission.[1] Under staged combustion condition locally fuel rich zones develop in the flame in which fuel bound nitrogen species react with NO to produce molecular nitrogen. The conversion degree of which the FBN (fuel bound nitrogen) conversion to N_2 is successful is determined by the thermodynamics of the system, and the rate of reactions in the fuel rich flame zone.[2,3]

The nitrogeneous compounds in the reducing zone may have two different origins:

In the first one of air two staging, they reacts in rich flames to form intermediates such as NH_3 and HCN in post-